A Wideband Compact Model for Integrated Inductors

Kok-Yan Lee, *Student Member, IEEE*, Saeed Mohammadi, *Senior Member, IEEE*, P. K. Bhattacharya, *Fellow, IEEE*, and Linda P. B. Katehi, *Fellow, IEEE*

***Abstract*—This letter presents a compact inductor model that is accurate beyond the inductor's self-resonance frequency. The inductor is represented as a short-circuited transmission line, whose impedance is a hyperbolic tangent function. This function is expanded to its third-order continued fractions approximation. The approximation results in a compact equivalent circuit model with frequency independent parameters that can be extracted directly from S-parameter measurements. No optimization is necessary in this process. The developed compact wideband inductor model is extremely useful for accurate transient and harmonic balance simulations where out of band response is important.**

***Index Terms*—Equivalent circuit model, integrated inductors, quality factor, self-resonance frequency, spiral inductors.**

I. Introduction

INTEGRATED spiral inductors are important components of radio frequency circuits. They are used as part of matching networks, filters and passive LC resonators. They suffer from poor quality factor Q due to frequency-dependent loss effects such as skin effect, eddy current loss in the substrate and current crowding.

For circuit analysis using CAD tools, it is essential to develop inductor models verified against measured results. The most common inductor model is the standard π-model with frequency independent lumped elements [1], [2]. While this model is useful over a limited frequency range, it does not properly model the distributed effects, proximity effects, or the higher-order loss effects and capacitive coupling. The conventional π-model has been extended with frequency-dependent lumped elements [1], [3]–[9]. The resulting models do a better job of describing the higher-order frequency effects, but cannot be easily implemented in time domain simulators. There are also alternative models such as distributed models and other lumped models that try to address the high frequency effects [1], [10]–[12]. A model based on a simple transmission line without any substrate effects is mentioned by Pucel [13].

This letter presents a new comprehensive modeling methodology for integrated inductors based on transmission line concept [14]. To the author's best knowledge, the model developed here is the only model with accurate response beyond inductor's first self-resonance frequency without need for optimization. The model is very simple and consists entirely of ideal frequency independent lumped elements suitable for time-domain transient analysis (SPICE) or harmonic balance nonlinear simulation. Model parameters are extracted from measured S-parameter data without a need for optimization. Model development and equivalent circuit parameters extraction are described in the following section. Section III discusses the accuracy of the model while Section IV concludes the letter.

Manuscript received January 28, 2006; revised May 18, 2006.

The authors are with the School of Electrical and Computer Engineering, Purdue University, West Lafayette, IN 47907 USA (e-mail: saeedm@purdue.edu).

A color version of Fig. 3 is available online at http://ieeexplore.ieee.org.

Digital Object Identifier 10.1109/LMWC.2006.880712

II. Model Development and Parameter Extraction

Assuming a standard π model, the extrinsic shunt pad admittances of inductors (Y_{ext1} and Y_{ext1}) are first extracted at relatively low frequencies. This is done by converting the S-parameter data to ABCD matrix. The relation between the ABCD matrix and components of the π model is given by

$$ABCD_{\text{complete}} = \begin{bmatrix} 1+\frac{Y_{\text{ext2}}}{Y_{\text{ind}}} & \frac{1}{Y_{\text{ind}}} \\ Y_{\text{ext1}}+Y_{\text{ext2}}+\frac{Y_{\text{ext1}}Y_{\text{ext2}}}{Y_{\text{ind}}} & 1+\frac{Y_{\text{ext1}}}{Y_{\text{ind}}} \end{bmatrix} \tag{1}$$

where $Z_{\text{ind}} = 1/Y_{\text{ind}} = B_{\text{complete}}$ is the impedance of the intrinsic inductor. Next, the inductor impedance is modeled as a short-circuit transmission line

$$Z_{\text{ind}} = Z_0 \tanh(\gamma l) \tag{2}$$

where l is the length of the transmission line (actual value is not needed), and Z_0 and γ are the characteristic impedance and complex propagation constant of the transmission line, respectively. The short-circuited transmission line equation $tanh(\gamma l)$ is then approximated using the third-order continued fractions approximation given by

$$\tanh(\gamma l) = \frac{(\gamma l)}{1+\frac{(\gamma l)^2}{3+\frac{(\gamma l)^2}{5+\cdots}}} \tag{3}$$

where

$$\gamma = \sqrt{(R+j\omega L)(G+j\omega C)}, \quad Z_0 = \sqrt{\frac{(R+j\omega L)}{(G+j\omega C)}}. \tag{4}$$

In the above equation, C is the shunt capacitance per unit length in F/m, L is the series inductance per unit length in H/m, R is the series resistance per unit length in Ω/m, and G is the shunt conductance per unit length in S/m. By substituting (3) and (4) in (2), one obtains the parameters of the intrinsic inductor model Z_{ind}

$$Z_{\text{ind}} = \frac{1}{Y_1+Y_2} \text{ where } Y_1 = \frac{1}{Rl+j\omega Ll}, \quad Y_2 = \frac{1}{Z_3+Z_4},$$
$$Z_3 = \frac{3}{(Gl+j\omega Cl)}, \quad Z_4 = \frac{1}{5}(Rl+j\omega Ll). \tag{5}$$

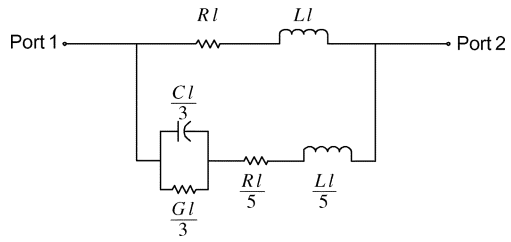

Fig. 1. Third-order transmission line circuit model of intrinsic inductors.

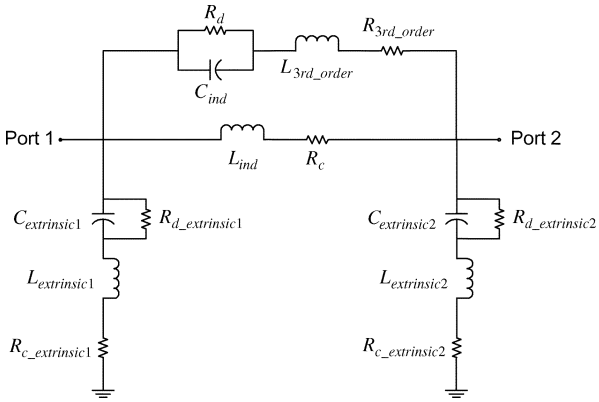

Fig. 2. Complete inductor equivalent circuit model based on third-order intrinsic inductor representation and second-order extrinsic admittance representation.

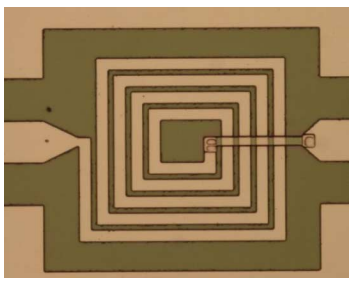

Fig. 3. Photomicrographs of fabricated 4.5-turn spiral inductor.

The intrinsic inductor model based on an ideal short-circuit transmission line is shown in Fig. 1. Using this model and by applying the same technique to represent the extrinsic admittances ($Y_{\rm ext1}$ and $Y_{\rm ext1}$) to their second-order continued fraction approximation [14], the complete inductor equivalent circuit model can be constructed. Fig. 2 shows the complete inductor model developed using this approach and considers coupling and other parasitic effects by replacing Ll with $L_{\rm ind}$, $Cl/3$ with $C_{\rm ind}$, $3/(Gl)$ with R_d, and Rl with R_c.

Spiral inductors with three different number of turns (1.5, 3.5, and 4.5 turns) were fabricated on high resistivity Si with a 1-μm lower CrAu metal and a 2-μm top metal. 7500 Å SiO_2 was used as the dielectric separating the two metals. Fig. 3 shows the fabricated 4.5-turn inductor in this technology.

In order to construct the equivalent circuit model, one can linearize both real and imaginary part of the inductor intrinsic admittance. The accuracy of the linearization approximation is improved at frequencies where $(\omega L_{\rm ind}/R_c)^2 \gg 1$ and less than the first resonance for the second-order model parameters and $(\omega R_d C_{\rm ind})^2 \gg 1$ and greater than the first resonance for the

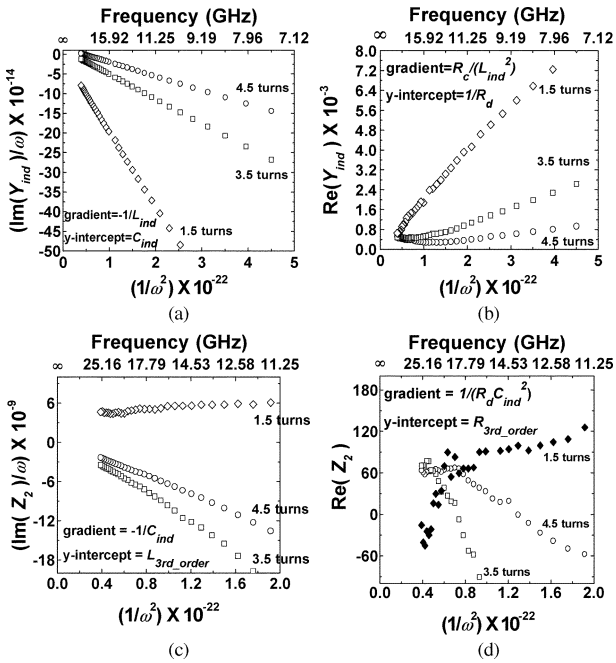

Fig. 4. Graphical method to extract (a) $L_{\rm ind}$, (b) R_c, (c) $L_{\rm third\_order}$ and $C_{\rm ind}$, and (d) $R_{\rm third\_order}$ and R_d of three different inductors from measured $Y_{\rm ind}$. $Y_{\rm ind}$ is extracted from S-parameter according to (1).

third-order model parameters. One can find linearized model parameters using the following:

$$\mathrm{Re}(Y_{\rm ind}) \approx \frac{R_c}{L_{\rm ind}^2}\frac{1}{\omega^2} + \frac{1}{R_d} \tag{6a}$$

$$\frac{\mathrm{Im}(Y_{\rm ind})}{\omega} \approx -\frac{1}{L_{\rm ind}}\frac{1}{\omega^2} + C_{\rm ind} \tag{6b}$$

$$\mathrm{Re}(Z_2) \approx R_{3rd\_order} + \frac{1}{R_d C_{\rm ind}^2}\frac{1}{\omega^2} \tag{6c}$$

$$\frac{\mathrm{Im}(Z_2)}{\omega} \approx L_{3rd\_order} - \frac{1}{C_{\rm ind}}\frac{1}{\omega^2} \tag{6d}$$

where $Z_2 = 1/Y_2$ is an intermediate impedance term defined in (5).

Equation (6) can be plotted as functions of angular frequency ω to extract $L_{\rm ind}$, $C_{\rm ind}$, R_c, R_d, $R_{\rm third\_order}$ and $L_{\rm third\_order}$ as shown in Fig. 4. The extrinsic admittances of the complete inductor model can be found using second-order continued fractions approximations of open-circuited admittance functions ($tanh$ function). Parameter extractions for the extrinsic elements are done using a similar approach to the one shown in Fig. 4. Table I shows the extracted parameters of the equivalent circuit models for the three inductors studied here. For a 1.5-turn inductor, since the self resonance frequency is higher than 26 GHz (maximum measured frequency), a simple first-order model is sufficient.

III. Results and Discussions

Fig. 5 shows the real and imaginary part of the measured and modeled inductors studied here. The models match the measured results beyond the inductor's self resonance frequency except for 1.5-turn inductor whose self resonance frequency is above the maximum measured frequency of 26 GHz. This is

TABLE I
COMPLETE MODELS FOR SPIRAL INDUCTORS STUDIED IN THIS WORK

Model parameters	4.5 turns	3.5 turns	1.5 turns
C_{ind} fF	14.58	12.58	3.71
L_{ind} nH	2.83	1.59	0.51
R_{sl} kΩ	-5.2	-3.6	-7.3
R_c Ω	17.5	13.9	5.4
R_{3rd_order} Ω	113.6	161.0	Not needed
L_{3rd_order} nH	0.29	-0.12	Not needed
Input C_{ext} fF	40.3	29.6	15.6
Input L_{ext} nH	0.27	0.19	-0.05
Input R_{sl_ext} kΩ	5.9	5.7	893.7
Input R_{c_ext} Ω	3.2	2.4	19.2
Output C_{ext} fF	30.3	24.3	16.3
Output L_{ext} nH	0.035	0.10	-0.06
Output R_{sl_ext} kΩ	-9.75	-3.94	15.14
Output R_{c_ext} Ω	3.75	11.31	17.07

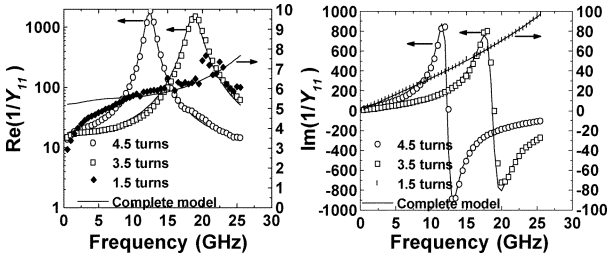

Fig. 5. Comparison of the measured and modeled $Re(1/Y_{11})$ and $Im(1/Y_{11})$.

achieved despite the fact that equivalent circuit parameters are extracted without any optimization.

Since our model formulation is derived from standard transmission line model as shown by (4), the components of the equivalent circuit model are directly related to the attenuation constant of the transmission line given by the real part of γ, and also to the phase constant given the by imaginary part of γ. As can be seen from Table I, some of the extracted parameters are components with negative values. Generally, negative component values are non-physical and therefore set to zero or ∞. However, in our model, negative component values are not necessarily non-physical as long as both real and imaginary parts of the attenuation constant γ are positive. The attenuation constant of these inductors is positive across the frequency range even with negative valued components thus satisfying the energy conservation law. Moreover, the phase constant is positive across the frequency range satisfying a forward traveling wave condition, except for the 1.5-turn inductor. In order to eliminate the non-physical parameter values extracted for the 1.5-turn inductor, we model it using a first-order intrinsic inductor model. From Fig. 5, one can see that the first-order intrinsic model that is used to model 1.5-turn inductor fits the measured results with excellent accuracy.

In summary, the accuracy of the model can be tested by assuring that the parameters are extracted from frequencies where the linearization approximation is valid. Furthermore, the validity of the model can be shown by plotting both real and imaginary part of γ and ensuring that they are both positive. If not, one needs to use a lower-order model. In general, a second-order model will be accurate to the first resonance and a third-order model is accurate beyond the first resonance.

IV. CONCLUSION

In conclusion, we have demonstrated a new modeling methodology for spiral inductors based on transmission line theory and continued fractions approximation. To the authors' best knowledge, this model is the first to report an excellent fit to the measured data beyond the resonance frequency. The wideband accuracy provided by this model is essential in simulating time domain transient response and also in the environment where the harmonic frequency response is important. The parameter extraction does not require any optimization and is accurate. We also show for the first time, the possibility of negative value components in the model and their relation to physical parameters of a transmission line; the attenuation constant and the phase constant.

REFERENCES

[1] J. R. Long and M. A. Copeland, "The modeling, characterization, and design of monolithic inductors for silicon rf ic's," *IEEE J. Solid-State Circ.*, vol. 32, no. 3, pp. 357–369, Mar. 1997.

[2] N. M. Nguyen and R. G. Meyer, "Si ic-compatible inductors and lc passive filters," *IEEE J. Solid State Circ.*, vol. 25, no. 4, pp. 1028–1031, Aug. 1990.

[3] J. N. Burghartz, M. Soyuer, and K. A. Jenkins, "Microwave inductors and capacitors in standard multilevel interconnect silicon technology," *IEEE Trans. Microw. Theory Tech.*, vol. 44, no. 1, pp. 100–104, Jan. 1996.

[4] E. Pettenpaul, H. Kapusta, A. Weisgerber, H. Mampe, J. Luginsland, and I. Wolff, "Cad models of lumped elements on gaas up to 18 ghz," *IEEE Trans. Microw. Theory Tech.*, vol. MTT-36, no. 2, pp. 294–304, Feb. 1988.

[5] J. R. Long and M. A. Copeland, "Modeling of monolithic inductors and transformers for silicon rfic design," in *IEEE MTT-S Int. Dig.*, 1995, pp. 129–134.

[6] S. Saimi, C. Joubert, and C. Glaize, "High frequency model for power electronics capacitors," *IEEE Trans. Power Electron.*, vol. 16, no. 2, pp. 157–166, Mar. 2001.

[7] B. Lakshminarayanan, H. C. Gordon, and T. M. Weller, "A substrate-dependent CAD model for ceramic multilayer capacitors," *IEEE Trans. Microw. Theory Tech.*, vol. 48, no. 10, pp. 1687–1693, Oct. 2000.

[8] W. Z. Cai, S. C. Shastri, M. Azam, C. Hoggatt, G. H. Loechelt, G. M. Grivna, Y. Wen, and S. Dow, "Development and extraction of high-frequency spice models for metal-insulator-metal capacitors," in *Proc. IEEE Int. Conf. Microelectron. Test Struct.*, Mar. 2004, vol. 17, pp. 231–234.

[9] S. S. Song, S. W. Lee, J. Gil, and H. Shin, "Simple wide-band metal-insulator-metal (MIM) capacitor model for RF applications and effect of substrate grounded shields," *Jpn. J. Appl. Phys.*, vol. 43, no. 4B, pp. 1746–1751, 2004.

[10] I. J. Bahl, "High-performance inductors," *IEEE Trans. Microw. Theory Tech.*, vol. 49, no. 4, pp. 654–664, Apr. 2001.

[11] L. Heinemann, R. Schulze, P. Wallmeier, and H. Grotstollen, "Modeling of high frequency inductors," in *Proc. IEEE Power Electron. Spec. Conf.*, 1994, vol. 2, pp. 876–883.

[12] T. Kamgaing, T. Myers, M. Petras, and M. Miller, "Modeling of frequency dependent losses in two-port and three-port inductors on silicon," in *Proc. IEEE Radio Freq. Integr. Circ. Symp.*, 2002, pp. 307–310.

[13] R. A. Pucel, "Design considerations for monolithic microwave circuits," *IEEE Trans. Microw. Theory Tech.*, vol. MTT-29, no. 6, pp. 513–534, Jun. 1981.

[14] K. Lee, S. Mohammadi, P. K. Bhattacharya, and L. P. B. Katehi, "Scalable compact models for embedded passives," in *Proc. 34th Eur. Microw. Conf.*, Paris, France, Oct. 2005, [CD ROM].